# Classical theory for the in-plane scattering of atoms from corrugated surfaces: Application to the Ar–Ag(111) system

Eli Pollak and Salvador Miret-Artés

Citation: J. Chem. Phys. **130**, 194710 (2009); doi: 10.1063/1.3131182
View online: http://dx.doi.org/10.1063/1.3131182
View Table of Contents: http://jcp.aip.org/resource/1/JCPSA6/v130/i19
Published by the American Institute of Physics.

# Classical theory for the in-plane scattering of atoms from corrugated surfaces: Application to the Ar–Ag(111) system

Eli Pollak[1,a)] and Salvador Miret-Artés[2]
[1]*Department of Chemical Physics, Weizmann Institute of Science, 76100 Rehovoth, Israel*
[2]*Instituto de Física Fundamental, Consejo Superior de Investigaciones Científicas, Serrano 123, 28006 Madrid, Spain*

(Received 18 February 2009; accepted 19 April 2009; published online 21 May 2009)

A classical Wigner in-plane atom surface scattering perturbation theory within the generalized Langevin equation formalism is proposed and discussed with applications to the Ar–Ag(111) system. The theory generalizes the well-known formula of Brako as well as the "washboard model." Explicit expressions are derived for the joint angular and final momentum distributions, joint final energy, and angular distributions as well as average energy losses to the surface. The theory provides insight into the intertwining between the energy loss and angular dependence of the scattering. At low energies the energy loss in the horizontal direction is expected to be large, leading to a shift of the maximum of the angular distribution to subspecular angles, while at high energies the energy loss in the vertical direction dominates, leading to a superspecular maximum in the angular distribution. The same effect underlies the negative slope of the average final (relative) energy versus scattering angle at low energies which becomes positive at high energies. The theory also predicts that the full width at half maximum of the angular distribution varies as the square root of the temperature. We show how the theory provides insight into the experimental results for scattering of Ar from the Ag(111) surface. © *2009 American Institute of Physics*.
[DOI: 10.1063/1.3131182]

## I. INTRODUCTION

The scattering of rare gas atoms by metal surfaces continues to be of both theoretical[1,2] and experimental interest.[3] Recent reviews may be found in Refs. 4–6. Much interest has focused on quantum diffraction, which appears even for atoms as heavy as Ar.[7,8] However, most of the features measured for the scattering of heavy atoms are classical in nature.[9–11] It is thus of interest to further develop the classical mechanics theory of atom surface scattering. There are a number of major features which any theory should account for. One is the rainbow structure of the angular distribution. This leads to a typical two peaked distribution whose minimum lies around the specular scattering angle. The second feature is the broadening of the distribution which is due to the interaction of the projectile with the surface and bulk phonons. The third and fourth features have to do with the angular dependence of the energy transfer to the surface and the angle dependent sticking probability, respectively.

Raukema *et al.*[12] undertook a detailed experimental study of the scattering of Ar (and $N_2$ and $O_2$) with the Ag(111) surface. They studied the incident energy and surface temperature dependence of the angular distribution as well as the angular and surface temperature dependences of the average energy loss to the surface. Perhaps the most challenging result to theory is their observations on the energy loss. They find that the relative energy loss (the ratio of the energy loss to the incident energy) around the peak of the scattered angular distribution is independent of the incident energy. Moreover, the slope of the relative final energy changes from negative to positive as one increases the incident energy. This behavior does not agree with models based on parallel momentum conservation and hard sphere scattering. A similar reversal of the slope in the angular dependence of the relative energy loss was observed earlier by Rettner *et al.* in their experimental studies of the scattering of Xe on a Pt(111) surface.[13]

The theoretical challenges raised by these results were also addressed in the context of detailed molecular dynamics studies. Barker *et al.*[14] undertook a molecular dynamics simulation which agreed with their experimental results on the scattering of Xe on Pt(111). The simulation results of Lahaye *et al.*[15] also accurately reflected the experimental observations for the scattering of Ar on Ag(111), including the observations on the energy loss and its energy and angular dependence. However, all these simulations are similar to the experimental results in that they do not provide an explanation or deep insight as to why does the slope of the relative final energy change with incident energy. In this present paper we will provide a rather simple classical theory which provides an understanding of these phenomena.

The classical theory of atom surface scattering has a long history. Brako[16] developed a classical model in which the vertical motion ($z$ direction) is coupled linearly to the phonon bath of the surface. He derived an analytical expression for the angular distribution, as well as for the energy and momentum transfer. His theory served as the basis for many theoretical studies of the scattering, especially by Hayes *et al.*[1,2] However, Brako did not include in his theory any

a)Electronic mail: eli.pollak@weizmann.ac.il.

 

corrugation and so he could not account directly for the rainbow phenomena. As a result he also ignored the coupling between the phonon bath and the horizontal motion of the atom along the surface. The classical rainbow effect which is caused by surface corrugation was then studied by Horn *et al.*[17] but they did not derive an explicit expression for the angular distribution which accounted for the double peaked structure. The first model which provided real insight into the effect of the corrugation is the so called "washboard model" of Tully[18] which was further extended in a more recent paper in Ref. 19. However, as in the analysis of Horn *et al.* the washboard model assumes an impulsive collision of the projectile with the surface.

We have recently formulated a classical theory for the angular distribution which takes into account the continuous interaction of the projectile with the surface.[20] It also included the interaction of the projectile with the surface phonons through the motion along the horizontal direction. The theory was based on the classical Wigner approach[21–24] (also known as "mixed quantum classical theory"[25,26] or the "linearization approximation"[27,28]) to molecular dynamics. The initial conditions of the phonon bath and the incident wavepacket may be treated quantum mechanically while the ensuing dynamics is obtained from the classical equations of motion.

In this present paper we significantly improve upon our previous treatment.[20] Since we limit ourselves to in-plane scattering, we can limit the theory to two degrees of freedom—the vertical and horizontal degrees of freedom. We include both vertical and horizontal couplings to the phonon bath. Not less important is that the coupling to the horizontal phonon bath used in this paper is translationally invariant and so presents a more realistic model for the collision dynamics than the model used in our previous treatment. Third, we extend the theory to include the angle and energy dependent distribution and so are able to account for the angular dependence of the average energy loss to the surface. For the sake of simplicity, we use here only a classical bath, thermal quantum effects are in any case negligible when considering a system such as Ar atoms scattering from a silver surface. In the present treatment we also ignore the sticking probability, which is a reasonable assumption when the incident energy is sufficiently large and the incident scattering angle is not too large.

The theory, including interaction of both projectile degrees of freedom with the surface is outlined in Sec. II, technical details may be found in Appendixes A thru C. Comparison and analysis of the experimentally measured results for the in-plane scattering of Ar from a Ag(111) surface is presented in Sec. III. We end with a discussion and suggestions for further improvements and generalizations of the present two dimensional theory.

## II. THEORETICAL FRAMEWORK

### A. The model Hamiltonian

As already mentioned in Sec. I, we limit ourselves to in plane scattering so that only two degrees of freedom have to be considered, the vertical distance $z$ and the horizontal coordinate $x$. The interaction potential $V(x,z)$ is mainly a function of the instantaneous vertical distance of the atom from the surface. Typically the surface is corrugated so that this distance is modulated periodically by the corrugation function $h(x)$. In the simplest possible approximation, the corrugation function is considered to be a cos (or a sin) function of the horizontal distances. Therefore the form we shall use throughout this paper for the interaction potential of the atom (whose mass is $M$) with the surface in the absence of fluctuations will be

$$V(x,z) = \bar{V}(z) + h\bar{V}'(z)\cos\left(\frac{2\pi x}{l}\right), \tag{2.1}$$

where $h$ is the corrugation depth in the horizontal direction. The vertical potential $\bar{V}(z)$ is assumed to be characterized by a binding energy $V_0$ of the incident particle to the surface. We assume that the corrugation is weak, that is $h$ is much smaller than the lattice lengths $l$, or the characteristic length scale associated with the vertical potential.

We further assume that both the vertical and horizontal coordinates fluctuate due to interaction with the thermal phonon bath of the surface. When the particle is bound to the surface, it diffuses freely along the horizontal direction. Its equation of motion in the horizontal direction is then the standard Langevin equation with a periodic potential. However, when the particle is far away from the surface, the interaction of the horizontal coordinate with the phonon bath vanishes. It is therefore reasonable to model the interaction of the horizontal motion with the phonon bath through a linear coupling between the horizontal coordinate and the bath which is modulated by a space dependent function $g(z)$ which vanishes when the horizontal coordinate is large. For the vertical motion we note that in the presence of the phonon bath, the vertical coordinate fluctuates, so that one should consider the interaction potential of the incident atom with the surface to be $\bar{V}(z-\delta z)$. Allowing only small fluctuations

$$\bar{V}(z-\delta z) \simeq \bar{V}(z) - \delta z\frac{d\bar{V}(z)}{dz}. \tag{2.2}$$

leads us to assuming that the Hamiltonian governing the scattering event is

$$\begin{aligned} H = {} & \frac{p_x^2+p_z^2}{2M} + \bar{V}(z) + \bar{V}'(z)h\cos\left(\frac{2\pi x}{l}\right) \\ & + \frac{1}{2}\sum_{j=1}^{N}\left[p_{j_z}^2 + \omega_{j_z}^2\left(x_{j_z} - \frac{c_{j_z}\sqrt{M}}{\omega_{j_z}^2}\bar{V}'(z)\right)^2\right] \\ & + \frac{1}{2}\sum_{j=1}^{N}\left[p_{j_x}^2 + \omega_{j_x}^2\left(x_{j_x} - \frac{c_{j_x}\sqrt{M}}{\omega_{j_x}^2}\frac{l}{2\pi}\sin\left(\frac{2\pi x}{l}\right)g(z)\right)^2\right]. \end{aligned} \tag{2.3}$$

The system momenta are $p_x$ and $p_z$ for the horizontal and vertical coordinates of the projectile, respectively. The horizontal and vertical bath degrees of freedom are characterized by the mass weighted momenta and coordinates $p_{j_i}$, $x_{j_i}$, $j$

$=1,\ldots,N$;
$i=x,z$.

The term coupling the horizontal motion to the respective phonon bath is periodic in the horizontal coordinate, this is necessary to assure the translational invariance of the model. When the particle is far from the surface it does not interact with the phonons, so that the bath Hamiltonian (in mass weighted coordinates and momenta) is defined to be

$$H_B = \frac{1}{2}\sum_{j=1,i=x,z}^{N}(p_{j_i}^2 + \omega_{j_i}^2 x_{j_i}^2). \tag{2.4}$$

### B. The distribution of final momenta

The incident atom is described by a Gaussian wave function $|\psi\rangle$. The quantum mechanical expression for the probability of finding the scattered atom with final momenta $p_x$ and $p_z$ is

$$\begin{aligned} P(p_x,p_z) &= \lim_{t\to\infty} P(p_x,p_z,t) \\ &= \lim_{t\to\infty} \mathrm{Tr}\left(\frac{e^{-\beta\hat{H}_B}}{Z_B}|\psi\rangle\langle\psi|\hat{K}^{\dagger}(t)\,\delta(p_x-\hat{p}_x)\right. \\ &\quad \left.\times\,\delta(p_z-\hat{p}_z)\hat{K}(t)\right), \end{aligned} \tag{2.5}$$

where the hats denote quantum operators, $\hat{K}(t)$ is the quantum propagator ($\hat{K}(t)=\exp((-i\hat{H}t/\hbar))$), and $\delta(x)$ is the Dirac "delta" function. The angular operator is defined as the angle with respect to the normal to the surface:

$$\hat{\theta} = \tan^{-1}\left(\frac{\hat{p}_x}{\hat{p}_z}\right). \tag{2.6}$$

The final momentum distribution in the Wigner representation takes the form

$$\begin{aligned} P(\bar{p}_x,\bar{p}_z) &= \lim_{t\to\infty}\int_{-\infty}^{\infty}\prod_{j=1,i=x,z}^{N}\frac{dp_{j_i}dx_{j_i}}{2\pi\hbar}\int_{-\infty}^{\infty}dp_x dp_z dx dz \\ &\quad\times\rho_{B,W}(\mathbf{p},\mathbf{x})\rho_S(p_x,p_z,x,z)\,\delta(\bar{p}_x-p_x(t))\,\delta(\bar{p}_z-p_z(t)), \end{aligned} \tag{2.7}$$

where the notation $p_z(t)$, $p_x(t)$ stands for the time evolution. In the classical limit the distribution function for the thermal harmonic baths is

$$\begin{aligned} \rho_{B,W}(\mathbf{p},\mathbf{x}) &\equiv \left\langle\frac{e^{-\beta H_B}}{Z_B}\right\rangle_W \\ &= \prod_{j=1,i=x,z}^{N}\left(\frac{\beta\omega_{j_i}}{2\pi}\exp\left(-\frac{\beta}{2}(p_{j_i}^2+\omega_{j_i}^2 x_{j_i}^2)\right)\right). \end{aligned} \tag{2.8}$$

The Wigner representation for the incident Gaussian wave function is

$$\begin{aligned} \rho_S(p_x,p_z,x,z) &= \left(\frac{1}{\pi\hbar}\right)^2\exp\left(-\gamma[(x-x_0)^2+(z-z_0)^2]\right. \\ &\quad\left.-\frac{(p_x-p_{x_0})^2+(p_z-p_{z_0})^2}{\hbar^2\gamma}\right), \end{aligned} \tag{2.9}$$

where the momenta $p_{x_0}$ and $p_{z_0}$ define the incident scattering angle:

$$\theta_{i0} = \tan^{-1}\left(\frac{p_{x_0}}{p_{z_0}}\right) \tag{2.10}$$

and the radial initial momentum:

$$p_0^2 = 2ME_0 = p_{x_0}^2 + p_{z_0}^2. \tag{2.11}$$

In the classical Wigner approximation which will be considered henceforth in this paper, the time evolution in Eq. (2.7) is given by the classical equations of motion.

As is well known, for the linearly coupled harmonic baths the equations of motion in the continuum limit are generalized Langevin equations (GLEs). Introducing the spectral densities

$$J_i(\omega) = \frac{\pi}{2}\sum_{j=1}^{N}\frac{c_{j_i}^2}{\omega_{j_i}}\delta(\omega-\omega_{j_i}), \quad i=x,z, \tag{2.12}$$

and associated friction functions

$$\eta_i(t) = \frac{2}{\pi}\int_0^{\infty}d\omega\frac{J_i(\omega)}{\omega}\cos(\omega t), \quad i=x,z, \tag{2.13}$$

the GLE for the horizontal motion takes the form (as may be readily seen by using the known forced harmonic oscillator solution for the bath variables and inserting it into the equations of motion for the system degrees of freedom)

$$\begin{aligned} &\sqrt{M}F_x(t)\cos\left(\frac{2\pi x_t}{l}\right)g(z_t) \\ &\quad= M\ddot{x}_t + \frac{\partial V(x_t,z_t)}{\partial x_t} + M\cos\left(\frac{2\pi x_t}{l}\right)g(z_t)\int_{-t_0}^{t}dt'\,\eta_x(t-t') \\ &\qquad\times\left(\frac{d}{dt'}\left[\frac{l}{2\pi}\sin\left(\frac{2\pi x_{t'}}{l}\right)g(z_{t'})\right]\right). \end{aligned} \tag{2.14}$$

The GLE for the vertical motion is more complicated, but we will not need it explicitly in the theory developed below. We do note that the vertical motion is a function of the vertical friction function $\eta_z(t)$ and noise $F_z(t)$. We initiate trajectories at the time $-t_0$. The projectile is initially sufficiently distant from the surface, such that at the vicinity of $z_0$ all the coupling functions vanish and the motion is that of a free particle. The noise functions therefore depend only on the initial conditions of the respective phonon bath. We note that

$$F_i(t) = \sum_{j=1}^{N} c_{j_i}\left( x_{j_i} \cos[\omega_{j_i}(t+t_0)] + \frac{p_{j_i}}{\omega_{j_i}} \sin[\omega_{j_i}(t+t_0)] \right), \quad i = x,z, \tag{2.15}$$

and the noise functions obey the fluctuation dissipation relations:

$$\langle F_i(t_1) F_j(t_2) \rangle = \delta_{ij} \frac{M}{\beta} \eta_i(t_1 - t_2), \quad i,j = x,z, \tag{2.16}$$

where the averaging is over the thermal distribution associated with the classical bath Hamiltonian as given in Eq. (2.4).

### C. Classical perturbation theory

#### 1. The change in the final momenta

The derivation of an explicit expression for the angular distribution is predicated on the assumption of weak coupling. Both the coupling between the vertical and horizontal motions is weak due to the small corrugation, and the coupling to the respective baths is weak. These conditions are not too stringent when considering the motion of a rare gas projectile whose interaction with the surface and the phonons does not include any strong chemical interactions. A few steps lead to the final desired result. First we solve perturbatively for the motion in the horizontal direction, this gives the change in the horizontal momentum as affected by the collision. Then we obtain the change in the vertical momentum through energy conservation and accounting for the energy loss to the bath due to the coupling of the projectile's motion to the heat bath of the surface. It then remains to average over initial conditions for the system and the harmonic baths. The averaging over the system is carried out by taking the limit that the width parameter in the incident wavepacket $\gamma \to 0$. This is equivalent to assuming that the initial momenta of the projectile are sharply defined.

Typically the Debye frequency of the crystal is much larger than the frequency of motion of the projectile when bound to the surface. We may therefore safely assume that the friction functions are Ohmic:

$$\eta_i(t) = 2\eta_i \delta(t), \quad i = x,z. \tag{2.17}$$

The origin of time is chosen as the point at which the unperturbed trajectory in the vertical direction reaches the turning point ($z_{tp}$) so that at time $t=0$ the vertical velocity vanishes. We then need to consider the motion from the initial time $-t_0$ when the atom is far from the surface until the time $t_0$ when it is again far from the surface. With this construction, the unperturbed trajectory in the vertical direction is an even function of time. To first order in the corrugation height $h$ and the noise strength, using the fact that initially the particle is far from the surface so that the coupling function $V'(z) = 0$, and that it is symmetric with respect to time, following the same derivation as given in Ref. 20, we find from the GLE [Eq. (2.14)] that the final momentum in the horizontal direction is given by the expression

$$p_x(t_0) \simeq p_x + p_z K(p_x,p_z) \sin\left( \frac{2\pi}{l}\left[ x + \frac{p_x}{M} t_0 \right] \right) + \Delta p_{x,1} + \Delta p_{x,2} \equiv p_x + \delta p_x, \tag{2.18}$$

where the friction induced momentum shift is (after an integration by parts):

$$\Delta p_{x,1} = -\eta_x \frac{p_x}{2} \int_{-t_0}^{t_0} dt g^2(z_t) \tag{2.19}$$

and the noise induced momentum shift is

$$\Delta p_{x,2} = \sqrt{M}\left( \cos\left( \frac{2\pi}{l} x(t_0) \right) \sum_{j=1}^{N} c_{j_x} X_{jc} x_{j_x}(t_0) + \sin\left( \frac{2\pi}{l} x(t_0) \right) \sum_{j=1}^{N} c_{j_x} \frac{X_{js}}{\omega_{j_x}} p_{j_x}(t_0) \right) \equiv \cos\left( \frac{2\pi}{l} x(t_0) \right) \Delta p_{x,2c} + \sin\left( \frac{2\pi}{l} x(t_0) \right) \Delta p_{x,2s}, \tag{2.20}$$

with

$$X_{jc} = \int_{-t_0}^{t_0} dt g(z_t) \left[ \cos\left( \frac{2\pi}{l} \frac{p_x}{M} t \right) \right] \cos(\omega_{j_x} t), \tag{2.21}$$

$$X_{js} = -\int_{-t_0}^{t_0} dt g(z_t) \sin\left( \frac{2\pi}{l} \frac{p_x}{M} t \right) \sin(\omega_{j_x} t), \tag{2.22}$$

and we used the notation:

$$x_{j_x}(t_0) = x_{j_x} \cos[\omega_{j_x} t_0] + \frac{p_{j_x}}{\omega_{j_x}} \sin[\omega_{j_x} t_0], \tag{2.23}$$

$$p_{j_x}(t_0) = -x_{j_x} \omega_{j_x} \sin[\omega_{j_x} t_0] + p_{j_x} \sin[\omega_{j_x} t_0]. \tag{2.24}$$

The unperturbed motion of the particle in the horizontal direction is that of a free particle, so that

$$x(t_0) = x + \frac{p_x}{M} t_0. \tag{2.25}$$

The "rainbow angle function" $K(p_x,p_z)$ is given in terms of the unperturbed dynamics as

$$K(p_x,p_z) = \frac{4\pi h}{l p_z} \int_0^{\infty} dt \cos\left( \frac{2\pi}{l} \frac{p_x}{M} t \right) \bar{V}'(z(t)). \tag{2.26}$$

The energy loss to the bath may be divided into two parts, an average energy loss and a fluctuational energy loss:

$$\Delta E_B = \sum_{i=x,z} (\langle \Delta E_B \rangle_i + \delta E_{B_i}). \tag{2.27}$$

As readily seen from Ref. 29, after some manipulation, one finds that for Ohmic friction, the average energy loss to the bath due to the motion in the $x$ direction is

$$\langle \Delta E_B \rangle_x = M \eta_x \frac{l^2}{4\pi^2} \int_{-t_0}^{t_0} dt \left( \frac{d}{dt} \left[ \sin\left( \frac{2\pi x_t}{l} \right) g(z_t) \right] \right)^2$$
$$\equiv \Delta\epsilon - \cos\left( \frac{4\pi}{l} x(t_0) \right) \Delta\epsilon_x, \tag{2.28}$$

where

$$\Delta\epsilon = E_0 \sin^2(\theta_{i0}) \eta_x \int_{-t_0}^{t_0} dt \left( g^2(z_t) + \frac{1}{\omega_x^2} \left( \frac{dg(z_t)}{dt} \right)^2 \right) \tag{2.29}$$

and

$$\Delta\epsilon_x = E_0 \sin^2(\theta_{i0}) \eta_x \int_{-t_0}^{t_0} dt \cos(2\omega_x t)$$
$$\times \left( g^2(z_t) + \frac{1}{\omega_x^2} \left( \frac{dg(z_t)}{dt} \right)^2 \right). \tag{2.30}$$

The "horizontal frequency parameter" is defined as

$$\omega_x = \frac{2\pi p_x}{lM}. \tag{2.31}$$

The fluctuational energy loss in the horizontal direction is then found to be

$$\delta E_{B_x} = -\sqrt{M} \frac{l}{2\pi} \int_{-t_0}^{t_0} dt \frac{d}{dt} \left[ \sin\left( \frac{2\pi x_t}{l} \right) g(z_t) \right] F_x(t)$$
$$= \sqrt{M} \frac{l}{2\pi} \left[ \sin\left( \frac{2\pi}{l} x(t_0) \right) \sum_{j=1}^{N} c_{j_x} X_{jc} p_{j_x}(t_0) \right.$$
$$\left. + \cos\left( \frac{2\pi}{l} x(t_0) \right) \sum_{j=1}^{N} c_{j_x} X_{js} \omega_{j_x} x_{j_x}(t_0) \right]$$
$$\equiv \sin\left( \frac{2\pi}{l} x(t_0) \right) \delta E_{B_x s} + \cos\left( \frac{2\pi}{l} x(t_0) \right) \delta E_{B_x c}. \tag{2.32}$$

One also readily finds that the variance of the fluctuational energy loss is proportional to the average energy loss:

$$\langle \delta E_{B_x} \rangle^2 = \frac{2}{\beta} \langle \Delta E_B \rangle_x. \tag{2.33}$$

Similar relations hold also for the vertical direction so that the average energy loss to the bath due to the vertical motion is (note that the dimension of $\eta_x$ is time$^{-1}$ while that of $\eta_z$ is time$^3$/mass$^2$):

$$\langle \Delta E_B \rangle_z = M \eta_z \int_{-t_0}^{t_0} dt \left( \frac{d\bar{V}'(z_t)}{dt} \right)^2 \equiv -\frac{p_z \Delta p_{z,1}}{M} \tag{2.34}$$

and the associated fluctuational energy loss is

$$\delta E_{B_z} = -\sqrt{M} \int_{-t_0}^{t_0} dt \frac{d\bar{V}'(z_t)}{dt} F_z(t)$$
$$= -\sqrt{M} \sum_{j=1}^{N} c_{j_z} \left( Z_{jc} x_{j_z}(t_0) + \frac{Z_{js}}{\omega_{j_z}} p_{j_z}(t_0) \right)$$
$$\equiv -\frac{p_z \Delta p_{z,2}}{M}, \tag{2.35}$$

where

$$Z_{jc} = \int_{-t_0}^{t_0} dt \frac{d\bar{V}'(z_{t+t_0})}{dt} \cos(\omega_{j_z} t) = 0, \tag{2.36}$$

$$Z_{js} = \int_{-t_0}^{t_0} dt \frac{d\bar{V}'(z_{t+t_0})}{dt} \sin(\omega_{j_z} t). \tag{2.37}$$

The variance of the vertical fluctuational energy loss obeys the same relation as for the horizontal energy loss:

$$\langle \delta E_{B_z} \rangle^2 = \frac{2}{\beta} \langle \Delta E_B \rangle_z. \tag{2.38}$$

The final momentum in the vertical direction is written down as

$$p_z(t_0) = -p_z + \delta p_z. \tag{2.39}$$

Energy conservation then implies that to first order

$$p_z \delta p_z = M \Delta E_B + p_x \delta p_x \tag{2.40}$$

so that we have derived within perturbation theory explicit expressions for the change in the final horizontal and vertical momenta.

### 2. The angular distribution

By definition, the angular distribution is

$$P(\theta) = \int_{-\infty}^{\infty} d\bar{p}_x d\bar{p}_z P(\bar{p}_x, \bar{p}_z) \delta\left( \theta - \tan^{-1}\left( \frac{\bar{p}_x}{\bar{p}_z} \right) \right). \tag{2.41}$$

Expanding to lowest order in the horizontal and vertical momentum shifts one finds that

$$\tan^{-1}\left( \frac{p_x(t_0)}{p_z(t_0)} \right) \simeq -\theta_{i0} + \delta\theta_i, \tag{2.42}$$

where

$$\delta\theta_i \equiv -\frac{\delta p_x}{p_z} - \frac{\cos^2(\theta_{i0})}{p_z^2} \frac{p_x}{p_z} M \Delta E_B. \tag{2.43}$$

Allowing the width parameter of the initial wavepacket to become arbitrarily small, and noting that the change in the final angle is independent of the initial value of the vertical coordinate we can carry out the integrations over the system momentum variables [see Eq. (2.7)] and the vertical coordinate to find that

$$P(\theta)=\frac{1}{l}\int_{-\infty}^{\infty}\prod_{j=1,i=x,z}^{N}\frac{dp_{j_i}dx_{j_i}}{2\pi\hbar}\rho_{B,W}(\mathbf{p},\mathbf{x})\times\int_0^l dx(t_0)\,\delta(\theta+\theta_{i0}-\delta\theta_i). \tag{2.44}$$

The integration over the bath variables is effected as in Ref. 20. One changes variables from the initial values of the bath coordinates at time $-t_0$ to their unperturbed values at the time $t=t_0$. More details are provided in Appendix A. One finds after some algebra that the angular distribution is given by the central expression:

$$P(\theta)=\frac{1}{l}\int_0^l dx(t_0)\frac{1}{\sqrt{\pi\Sigma^2(x(t_0))}}\exp\left(-\frac{\left(\theta+\theta_{i0}+K(p_x,p_z)\sin\left(\frac{2\pi}{l}x(t_0)\right)+\Delta\theta_1(x(t_0))\right)^2}{\Sigma^2(x(t_0))}\right). \tag{2.45}$$

The angular shift is found to be

$$\Delta\theta_1(x(t_0))=\tan(\theta_{i0})\left(\frac{\langle\Delta E_B\rangle}{2E_0}-\frac{\eta_x}{2}\int_{-t_0}^{t_0}dtg^2(z_t)\right) \tag{2.46}$$

and the variance is

$$\Sigma^2(x(t_0))=\frac{2\tan(\theta_{i0})}{\beta E_0}\left(\Delta\theta_1(x(t_0))+\eta_x\tan(\theta_{i0})\int_{-t_0}^{t_0}dtg^2(z_t)\left[1-\cos\left(\frac{4\pi}{l}x(t_0)\right)\right]\right)+\frac{\eta_x}{\beta E_0}\left(\int_{-t_0}^{t_0}dtg^2(z_t)\left[1+\frac{\cos\left(\frac{4\pi}{l}x(t_0)\right)\cos(2\omega_x t)}{\cos^2(\theta_{i0})}\right]\right). \tag{2.47}$$

The expression for the angular shift [Eq. (2.46)] is of special interest. It shows that the angular shift of the distribution can be either positive or negative. Since the incident angle $\theta_{i0}$ is by definition negative, the angular shift can be positive if the horizontal friction coefficient is sufficiently large. If the energy loss to the vertical bath is more important the angular shift will be negative. At high energies, one may expect that the vertical energy loss dominates, since the atom spends only a short time in the region of interaction with the surface and the fast vertical motion gives a hard impulse to the vertical phonons. Due to the fast motion, the particle hardly moves in the horizontal direction and the energy loss to the horizontal modes will be much smaller. In this case, the large vertical energy loss implies that the horizontal momentum will be decreased less than the vertical momentum so the angular distribution shifts toward angles that are larger then specular. Conversely, at low energies, the particle may move a long distance in the horizontal direction and the interaction with the horizontal phonon bath dominates so that the angular shift is positive. The loss of horizontal momentum then shifts the angular distribution to angles that are smaller than the specular angle.

### 3. Some interesting limits

The first limit to be considered is the "high horizontal frequency" limit. If the horizontal frequency $\omega_x$ is sufficiently large such that the time spent by the particle in the vertical direction is large compared to the horizontal period $(2\pi/\omega_x)$ one may expect that terms such as $\int_{-t_0}^{t_0}dtg^2(z_t)\cos(2\omega_x t)$ will be much smaller than terms such as $\int_{-t_0}^{t_0}dtg^2(z_t)$. In this limit, one may neglect the energy loss function $\Delta\epsilon_x$ [see Eq. (2.30)] as compared to the average energy loss $\Delta\epsilon$. This simplifies the analysis significantly, since now the angular shift function $\Delta\theta_1(x(t_0))$ becomes independent of the horizontal coordinate.

If there is no coupling to the baths then the shift $(\Delta\theta_1(x(t_0)))$ vanishes and one has

$$P(\theta)\to\frac{1}{\pi}\frac{H(K^2-(\theta+\theta_{i0})^2)}{\sqrt{K^2(p_0,\theta_{i0})-(\theta+\theta_{i0})^2}}, \tag{2.48}$$

where $H(x)$ is the Heaviside function, that is, one regains our previously derived result[20] for the angular distribution in the absence of dissipation.

In the absence of corrugation there is no energy loss in the horizontal direction and the lattice length $l$ diverges. One then obtains a shifted Gaussian angular distribution, shifted to angles which are larger than the specular angle as a result of the energy loss in the vertical direction:

$$P(\theta)\to\frac{1}{\sqrt{\pi\Sigma^2}}\exp\left(-\frac{(\theta+\theta_{i0}+\Delta\theta_1)^2}{\Sigma^2}\right)=\left(\frac{\beta E_0^2}{2\pi\tan^2(\theta_{i0})\langle\Delta E_B\rangle_z}\right)\times\exp\left(-\beta E_0^2\frac{\left(\theta+\theta_{i0}+\tan(\theta_{i0})\frac{\langle\Delta E_B\rangle_z}{2E_0}\right)^2}{\langle\Delta E_B\rangle_z\tan^2(\theta_{i0})}\right). \tag{2.49}$$

In this case, the angular shift $\Delta\theta_1$ is always negative and the angular distribution is centered about an angle that is greater than the specular angle since the momentum in the horizontal direction is conserved while the vertical momentum has become smaller in magnitude.

In the limit that the temperature goes to 0, the variances vanish, and Eq. (2.45) reduces (using the high horizontal frequency limit) to

$$P(\theta) \to \frac{1}{\pi}\frac{H(K^2-(\theta+\theta_{i0}+\Delta\theta_1)^2)}{\sqrt{K^2(p_0,\theta_{i0})-(\theta+\theta_{i0}+\Delta\theta_1)^2}}. \tag{2.50}$$

This is the so-called static limit, in which the corrugation of the potential still plays a role although the broadening from the phonon bath vanishes.

#### 4. The joint angle and energy distribution and the angle dependent final average energy

The joint probability distribution for finding the scattered atom at the scattering angle $\theta$ and final energy $E$ is by definition

$$P(\theta,E) = \frac{1}{l}\int_{-\infty}^{\infty}\prod_{j=1,i=x,z}^{N}\frac{dp_{j_i}dx_{j_i}}{2\pi\hbar}\rho_{B,W}(\mathbf{p},\mathbf{x}) \times\int_0^l dx(t_0)\,\delta(\theta+\theta_{i0}-\delta\theta_i)\,\delta(E-E_0+\Delta E). \tag{2.51}$$

As for the angular distribution, one can again carry out the thermal averaging as outlined in Appendix B, to find that the expression for the joint probability distribution is as given in Eq. (B8). The final energy distribution is obtained by integration over the angle and one readily finds

$$P(E) = \int_{-\pi/2}^{\pi/2} d\theta P(\theta,E) = \frac{1}{l}\int_0^l dx(t_0)\left(\frac{\beta}{4\pi\langle\Delta E_B\rangle}\right)^{1/2} \times\exp\left(-\frac{\beta}{4}\left[\frac{(E-E_0+\langle\Delta E_B\rangle)^2}{\langle\Delta E_B\rangle}\right]\right). \tag{2.52}$$

This result is a generalization of Brako's result. He did not include any corrugation, so that the average energy loss was independent of the horizontal coordinate. Here, due to the coupling of the horizontal mode to the phonon bath, the energy loss does depend on the horizontal coordinate. One must thus average over the energy loss distribution found for each value of the horizontal coordinate. In the high horizontal frequency limit, this dependence on the horizontal coordinate vanishes and one regains Brako's result.

Raukema *et al.*[12] measured the dependence of the final average energy of Ar scattered from the Ag(111) surface as a function of the final scattering angle. It is therefore of interest to write down the theoretical expression for the final angle dependent average energy $\langle E(\theta)\rangle$. Ignoring the possibility of sticking to the surface we have by definition that

$$\langle E(\theta)\rangle = \frac{\int_{-\infty}^{\infty} dEEP(\theta,E)}{P(\theta)}. \tag{2.53}$$

As shown in Appendix C, one then readily finds that the angle dependent final average energy is

$$\langle E(\theta)\rangle = (E_0 - \langle\langle\Delta E_B\rangle\rangle_l) + \frac{2}{\beta P(\theta)}\frac{\partial}{\partial\theta}\langle P(\theta)\Delta\theta_1(x(t_0))\rangle_l \tag{2.54}$$

and we used the notation for the averaging over the horizontal coordinate as in Eq. (C6). In the high horizontal frequency limit the shift $\Delta\theta_1(x(t_0))$ and the average energy loss are no longer dependent on the horizontal coordinate. The expression for the angle dependent final average energy simplifies to

$$\langle E(\theta)\rangle \simeq E_0 - \langle\Delta E_B\rangle + \frac{2\Delta\theta_1}{\beta}\frac{\partial\ln[P(\theta)]}{\partial\theta} \tag{2.55}$$

showing explicitly that the slope of the angle dependent final average will reflect the angular shift function. Especially if the rainbow angle function is not large, one may expect the angular distribution to be a bell shaped distribution such that around the peak its logarithmic derivative will be a decreasing function of the final angle. One then sees that when the angular shift is positive (low energy, large horizontal energy loss) the slope of $\langle E(\theta)\rangle$ with respect to the scattering angle will be negative while at high energies when the angular shift is expected to be negative, the slope will be positive. This is the qualitative behavior measured by Raukema *et al.*[12] in their study of the scattering of Ar on Ag(111) as analyzed in further detail in Sec. III. Moreover, at the peak of the angular distribution, the final average energy is just identical to the difference between the incident energy and the energy lost to the surface.

## III. CLASSICAL WIGNER THEORY FOR THE SCATTERING OF Ar FROM Ag(111)

Inspection of Fig. 11 of Ref. 12 leads to some interesting conclusions. They found that the relative final energy $(\langle E(\theta_{\max})\rangle/E_0)$ is the same around the peak of the angular distribution, irrespective of the incident energy. As already discussed above, $\langle E(\theta_{\max})\rangle$ is just the average energy loss to the surface. From the Langevin model we used, one notes that the average energy loss to the bath is independent of the surface temperature (this is also verified experimentally as may be seen from inspection of the temperature dependent results presented in Fig. 11 of the same reference) so that the relative final energy may be considered to be a constant parameter which is relevant to the system studied. For Ar scattering on Ag(111) one notes from the corresponding Fig. 11 that

$$\frac{\langle E\rangle}{E_0} = 0.75. \tag{3.1}$$

As already discussed in Sec. II, one expects that the angular shift function will be positive at low energies due to

the enhanced energy loss to the horizontal bath and negative at high energies due to the enhanced energy loss to the vertical bath. It is therefore a reasonable zeroth order guess to assume that this function is inversely proportional to the incident momentum. Furthermore, from the experimental results we notice that at the incident energy of 1060 meV, the angle dependent final average energy becomes independent of the angle. This will happen if the angular shift at this energy vanishes. We therefore assume that the angular shift function takes the form

$$\Delta\theta_1 = -\theta_1\left(1 - \sqrt{\frac{1060}{E}}\right), \tag{3.2}$$

where $\theta_1$ is for the time being a free positive parameter to be determined by fitting the theoretical expressions to the experimental results.

We then note that in the high horizontal frequency limit, knowledge of the average energy loss and the angular shift suffices to determine also the term $\eta_x\int_{-t_0}^{t_0} dtg^2(z_t)$ since

$$\eta_x\int_{-t_0}^{t_0} dtg^2(z_t) = \frac{\langle\Delta E_B\rangle}{E_0} - \frac{2\Delta\theta_1}{\tan(\theta_{i0})}. \tag{3.3}$$

To complete the theory we need to know the rainbow angle function and its energy dependence. However, from experiment, we note that at all energies and temperatures measured, the angular distributions are bell shaped and do not show the double peaked rainbow structure. This means that the rainbow function $K$ is much smaller than the variance $\Sigma$ and so it can be neglected. Finally the variance depends on the lattice length $l$ which is taken from Ref. 15 to be 2.8 Å (along the $[10\bar{1}]$ direction). We are thus left with a one parameter fit ($\theta_1$) to compare with the experimental results. Using the value $\theta_1 = 0.015$ (in radians) we find that the angle dependent final relative average energy is as shown in Fig. 1 for the same incident energies as studied experimentally by Raukema *et al.*[12] One notes that these results are in almost quantitative agreement with the experimental results.

The associated angular distributions are shown in Fig. 2. Here we note that qualitatively we find that the full width at half maximum (FWHM) decreases with energy, however, it does so much more rapidly than observed experimentally. At the low energy, the FWHM is too large (37° as compared to the experimental result of 34°) while at the highest energy the FWHM is too small (10° as compared to the experimental result of 22°). We also do not observe the very shallow minimum in the FWHM as a function of energy as observed in the experiments and the numerical simulations. There is also an additional discrepancy. Experimentally the maxima of the distributions were shifted to angles that are slightly larger than the specular angle. The theory we have used cannot account for this, as the maxima are determined by the angular shift function and it changes sign with energy indicating that at low energies the maximum in the angular distribution is at angles which are smaller than specular and only at higher energies is the maximum shifted to angles that are greater than the specular angle. This point is discussed further in Sec. IV.

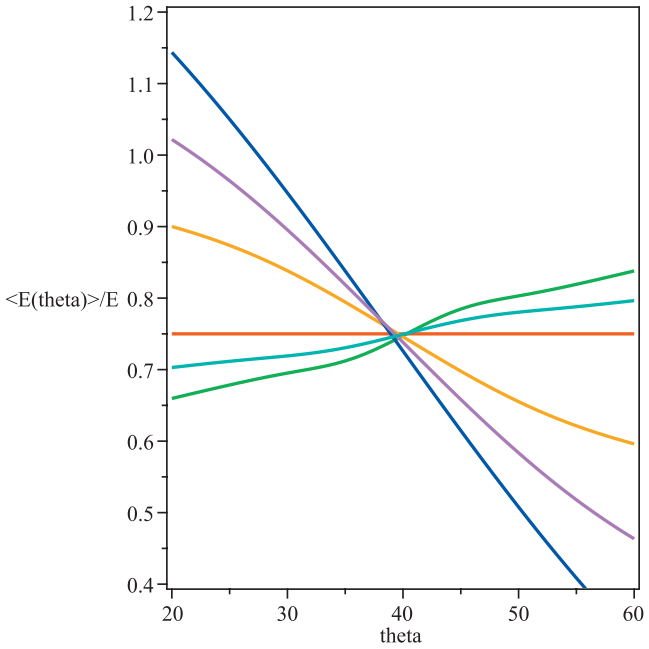


FIG. 1. (Color) Angular dependence of the relative final energy. The lines are for incidence energies of 210, 310, 480, 1060, 1580, and 2560 meV. The highest incidence energy is the lowest line at angles below the specular angle (40°), the other energies increase monotonically with decreasing incidence energy (at angles below specular). Note the change of slope at the incidence energy of 1060 meV.

Finally, Raukema *et al.*[12] also measured the temperature dependence of the angular distribution and the average final energy. In Fig. 3 we show the temperature dependence we find at the experimental energy of 1060 meV. As also seen experimentally, the FWHM of the distribution increases significantly with increasing temperature. Experimentally the FWHM changed from 24° at $T=800$ K to 16° at $T$

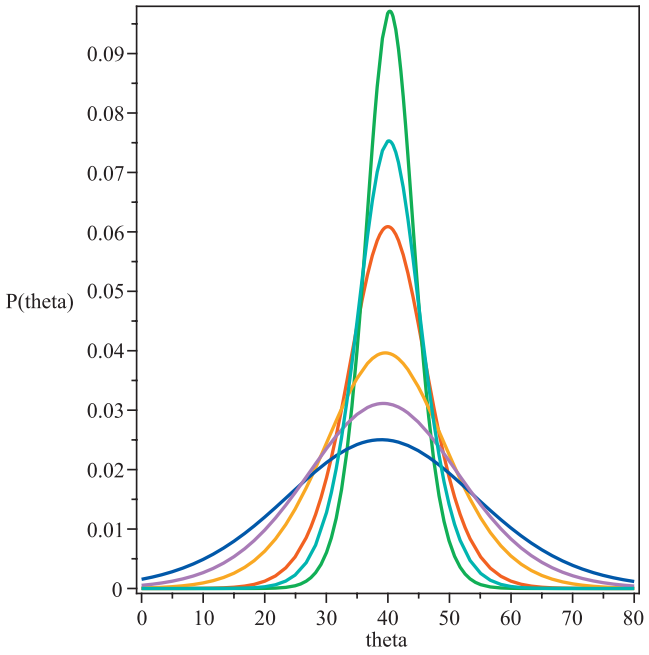


FIG. 2. (Color) Incidence energy dependence of the scattered angular distributions. The incidence energies are as in Fig. 1, the narrowest plot is for the highest energy, the width increases monotonically as the energy is decreased. The surface temperature is 600 K.

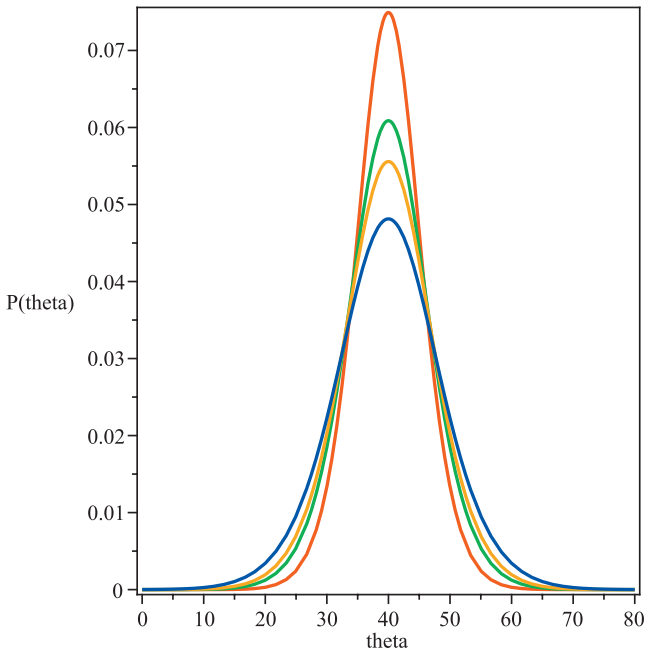


FIG. 3. (Color) Surface temperature dependence of the scattered angular distributions at an incidence energy of 1060 meV. The surface temperatures are 330, 500, 600, and 800 K. The broadest distribution is at the highest temperature and the width decreases with decreasing temperature.

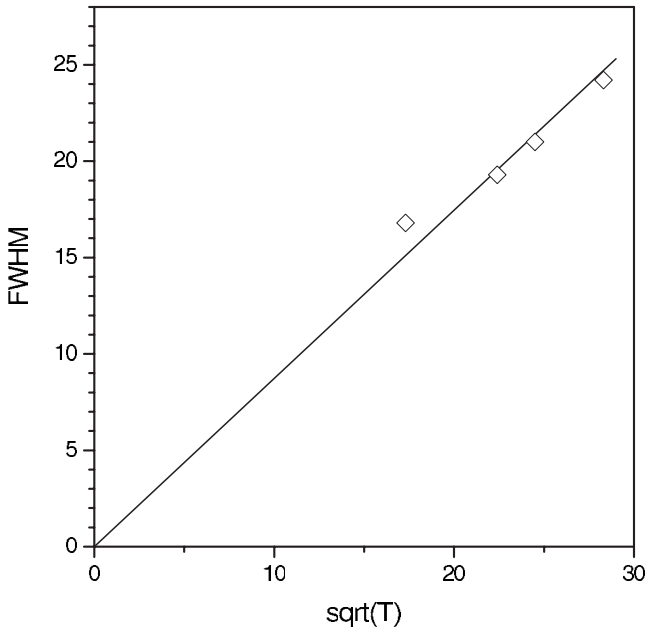


FIG. 4. Experimental square root dependence of the FWHM (in degrees) of the angular distribution on the surface temperature. The experimental widths are adapted from Ref. 12 and are plotted vs. the square root of the temperature. Note that they extrapolate nicely to 0 at $T=0$ K while if they are plotted on a linear scale as in Ref. 12 they extrapolate to a large constant (11°) which is unphysical.

$=330$ K. As may be inferred from Fig. 3 we find that the FWHM changes from 19° at $T=800$ K to 13° at $T=330$ K. Our theory predicts that the width increases as the square root of the temperature, while Raukema *et al.* indicate that it increases linearly with the temperature. However, inspection of their data and taking into consideration the experimental uncertainties shows that the experimental data can be reasonably well fitted to a square root dependence on the temperature as shown in Fig. 4. Finally, by construction, at this energy, the average energy is independent of the angle, as also observed experimentally.

## IV. DISCUSSION

In this paper we derived an improved version of the classical theory of in-plane atom surface scattering. Expressions were derived for the joint final energy and angular distribution, the angle dependent final average energy and the angular distribution. These expressions can be readily computed when using simple potentials such as a Morse oscillator potential for the vertical potential and a periodic cosine or sine potential for the horizontal motion. One of the interesting outcomes of the present study is a deeper understanding of the intertwining between energy loss and the angular dependence of the scattering. Our theoretical analysis points out that at low energies, the relative energy loss due to horizontal coupling is facilitated, while the opposite is true at high energies. As a result, at low energies subspecular scattering angles are preferred and vice versa at high energies. We noted that there is a direct relationship between the location of the maximum of the angular distribution and the extent of energy loss in the horizontal and vertical directions. When the relative energy loss in the vertical direction is larger than the horizontal, one should expect the maximum to be shifted to super specular angles and vice versa. These same effects come into play when studying the angle dependence of the final average energy. At low incidence energies one should expect the final average energy to decrease with increasing scattering angle and vice versa at high energies. We also showed how one can derive the temperature dependence for the FWHM of the angular distribution and showed that it increases as the square root of the temperature.

As an application of these results we chose to study the scattering of Ar from a Ag(111) surface. Our theory accounted well for the following experimental observations:

(a) The angular dependence of the final relative average energy. We showed that with a simple ansatz, the theory provides good agreement with the observed change in slope in the dependence of the average energy on the scattering angle as the incidence energy is increased.
(b) Our theory predicts that at the maximum of the angular distribution, the final average energy is just the overall average energy. The fact that experimentally this final relative average energy is the same irrespective of the incidence energy allowed us to conclude that the relative average energy loss for this system is 0.25. This number provides a universal like characterization of the scattering of Ar from the Ag(111) surface.
(c) The classical theory predicts that the width of the angular distribution decreases with increasing incidence energy, this result is in only partial agreement with experiment. We do note though that the experimental paper does not provide any information on the width of the initial energy distribution. The results we obtained

are valid only for sharply defined initial velocities. One should also remember that the present theory is derived for a very simple minded potential model for the interaction of the atom with the surface.

(d) We predict a square root temperature dependence of the FWHM of the angular distribution and showed that this prediction agrees well with the experimental results, even though Raukema *et al.* indicated that their FWHM temperature dependence is linear. In fact, the linear dependence leads to the conclusion that at $T=0$ K there is a substantial width. Our fit using the square root dependence leads to a vanishing width in this limit as is appropriate in the classical limit. It should be stressed that even within our classical theory, at $T=0$ K the corrugation does not disappear. The $T=0$ K limit is identical to the limit of a vanishing phonon bath, which is known also as the static limit. We also note that at $T=0$ K the bath should be treated quantum mechanically. One will then find a finite phonon induced width induced by the zero point fluctuations of the phonon bath. However, it will be very small and not in agreement with the extrapolated results of Ref. 12.

(e) The most glaring discrepancy between experiment and theory is in the location of the maximum of the angular distribution. The experimental results indicate that the maximum is a few degrees larger than the specular angle. Our theory predicts that the maximum will be lower than the specular angle at low energies and greater than the specular angle at high energies. The experimental asymmetry may be related to the fact that we assumed that the horizontal corrugation is symmetric with a single periodic term. Asymmetry in the distribution may be induced if the potential is ratchet like. In fact, the numerical investigations of Lahaye *et al.*[15] indicate that in the ($[11\bar{2}]$) direction the atoms of the second layer are not symmetrically displaced relative to those of the first layer. Moreover, the simulations were carried out along the symmetrical ($[10\bar{1}]$) direction, and they too did not give a shift which was in agreement with the experiment. There are other sources of asymmetry which we did not consider. These include the initial preparation, if for some reason the width in the initial distribution is different in the horizontal and vertical directions this would lead to an asymmetry in the final angular distribution. Finally, in the present simplified application of the theory to the Ar–Ag(111) system we assumed for the sake of simplification that the rainbow scattering can be ignored. In fact, the rainbow scattering may affect the angular distribution to some extent, even though the width of the distribution is substantially larger than the distance of the rainbow angle from the specular angle.

## ACKNOWLEDGMENTS

We thank Dr. J. Moix and Dr. S. Sengupta for fruitful discussions. We gratefully acknowledge support of this work by a grant of the Israel Science Foundation. S.M.-A. would like to thank the Ministry of Science and Innovation of Spain for a project with Reference No. FIS2007-62006.

## APPENDIX A: THERMAL AVERAGING

The dependence on the bath comes from the thermal distributions and the fluctuational terms $\Delta p_{x,2}$ and $\Delta p_{z,2}$. We introduce the following stochastic variables:

$$Y_s = \frac{\Delta p_{x,2s}}{p_z} + \frac{\cos^2(\theta_{i0})}{p_z^2}\frac{p_x}{p_z} M \delta E_{B_x s}, \tag{A1}$$

$$Y_c = \frac{\Delta p_{x,2c}}{p_z} + \frac{\cos^2(\theta_{i0})}{p_z^2}\frac{p_x}{p_z} M \delta E_{B_x c} \tag{A2}$$

and note the following thermal average, which is found by using the Fourier representation of the Dirac delta functions, inserting the explicit expressions for the various shifts as given in Eqs. (2.20) and (2.32):

$$\left\langle \delta\left(Y_s - \frac{\Delta p_{x,2s}}{p_z} - \frac{\cos^2(\theta_{i0})}{p_z^2}\frac{p_x}{p_z} M \delta E_{B_x s}\right) \delta\left(Y_c - \frac{\Delta p_{x,2c}}{p_z} - \frac{\cos^2(\theta_{i0})}{p_z^2}\frac{p_x}{p_z} M \delta E_{B_x c}\right)\right\rangle = \left(\frac{\beta p_z^2}{2\pi M\sqrt{S_s S_c}}\right)\exp\left(-\frac{\beta p_z^2}{2M}\left(\frac{Y_s^2}{S_s} + \frac{Y_c^2}{S_c}\right)\right). \tag{A3}$$

Here, we used the following notation:

$$S_s = \sum_{j=1}^{N} \frac{c_{j_x}^2}{\omega_{j_x}^2}\left(X_{js} + M\frac{\cos^2(\theta_{i0})}{p_z}\frac{p_x}{p_z}\frac{l}{2\pi}\omega_{j_x} X_{jc}\right)^2, \tag{A4}$$

$$S_c = \sum_{j=1}^{N} \frac{c_{j_x}^2}{\omega_j^2}\left(X_{jc} + M\frac{\cos^2(\theta_{i0})}{p_z}\frac{p_x}{p_z}\frac{l}{2\pi} X_{js}\omega_{j_x}\right)^2, \tag{A5}$$

$$S = S_s + S_c. \tag{A6}$$

Similarly for the vertical bath we note that

$$\langle \delta(P_z - \Delta p_{z,2})\rangle = \left(\frac{\sin^2(\theta_{i0})}{4\pi M E_0 \sigma_z^2}\right)^{1/2}\exp\left(-\frac{P_z^2 \sin^2(\theta_{i0})}{4ME_0\sigma_z^2}\right) \tag{A7}$$

and the vertical variance is found to be

$$\sigma_z^2 = \frac{M}{4\beta E_0^2}\tan^2(\theta_{i0})\sum_j \frac{c_{j_z}^2}{\omega_{j_z}^2}(Z_{jc}^2 + Z_{js}^2) = \frac{\langle \Delta E_B\rangle_z}{2\beta E_0^2}\tan^2(\theta_{i0}). \tag{A8}$$

Inserting these results in the expression for the angular distribution as given in Eq. (2.44), one finds the intermediate result (with $Z_i = Y_i/\sqrt{S_i}$, $i = s, c$):

$$P(\theta) = \int_0^l dx(t_0)\int_{-\infty}^{\infty} dZ_s dZ_c dP_z \left(\frac{\beta p_z^2}{2\pi M}\right)\left(\frac{\sin^2(\theta_{i0})}{4\pi M E_0 \sigma_z^2}\right)^{1/2} \times \exp\left(-\frac{\beta p_z^2}{2M}(Z_s^2 + Z_c^2)\right)\exp\left(-\frac{P_z^2 \sin^2(\theta_{i0})}{4ME_0\sigma_z^2}\right) \times \delta\left(\theta + \theta_{i0} + K(p_x, p_z)\sin\left(\frac{2\pi}{l}x(t_0)\right) + \sqrt{S}\bar{X} + \frac{\Delta p_{x,1}}{p_z} + \frac{\cos^2(\theta_{i0})}{p_z^2}\frac{p_x}{p_z}M\left(\langle \Delta E_B\rangle - \frac{p_z P_z}{M}\right)\right), \tag{A9}$$

where

$$\bar{X} = Z_s \sin(\phi)\sin\left(\frac{2\pi}{l}x(t_0)\right) + Z_c \cos(\phi)\cos\left(\frac{2\pi}{l}x(t_0)\right). \tag{A10}$$

One thus remains with the integration over the variables $Z_s$, $Z_c$, and $P_z$. These are carried out by defining the "angle":

$$\tan(\phi) = \sqrt{\frac{S_s}{S_c}} \tag{A11}$$

and the variable

$$\Delta X = -Z_s \cos(\phi)\cos\left(\frac{2\pi}{l}x(t_0)\right) + Z_c \sin(\phi)\sin\left(\frac{2\pi}{l}x(t_0)\right) \tag{A12}$$

so that

$$Z_s^2 + Z_c^2 = \frac{2(\Delta X^2 + \bar{X}^2)}{\left[\cos^2\left(\phi - \frac{2\pi}{l}x(t_0)\right) + \cos^2\left(\phi + \frac{2\pi}{l}x(t_0)\right)\right]} \tag{A13}$$

and

$$dZ_s dZ_c = d\bar{X}d\Delta X\left|\frac{2}{\left[\cos^2\left(\phi - \frac{2\pi}{l}x(t_0)\right) + \cos^2\left(\phi + \frac{2\pi}{l}x(t_0)\right)\right]}\right|. \tag{A14}$$

It is then a matter of some tedious Gaussian integrations to find that the expression for the angular distribution is

$$P(\theta) = \frac{1}{l}\int_0^l dx(t_0)\frac{1}{\sqrt{\pi\Sigma^2}}\int_{-\infty}^{\infty} dW \exp\left(-\frac{W^2}{\Sigma^2}\right) \times \delta\left(\theta + \theta_{i0} + K(p_x, p_z)\sin\left(\frac{2\pi}{l}x(t_0)\right) + \frac{\Delta p_{x,1}}{p_z} + \frac{\cos^2(\theta_{i0})}{p_z^2}\frac{p_x}{p_z}M\langle \Delta E_B\rangle + W\right) \tag{A15}$$

and the overall variance which is dependent on the horizontal coordinate is

$$\Sigma^2 = 2\sigma_z^2 + \frac{MS}{\beta p_z^2}\left[\cos^2\left(\phi - \frac{2\pi}{l}x(t_0)\right) + \cos^2\left(\phi + \frac{2\pi}{l}x(t_0)\right)\right]. \tag{A16}$$

It remains to provide the continuum limit expression. Using the symmetry in time of the unperturbed motion in the vertical direction, one finds after some algebra the following identities:

$$S_c = \eta_x\int_{-t_0}^{t_0} dt[\cos(2\theta_{i0}) + \cos(2\omega_x t)]g^2(z_t) + \frac{\sin^2(\theta_{i0})}{E_0}(\Delta\epsilon - \Delta\epsilon_x), \tag{A17}$$

$$S_s = \eta_x\int_{-t_0}^{t_0} dt g^2(z_t)[(1 + 2\sin^2(\theta_{i0}) - \cos(2\omega_x t))] + \frac{\sin^2(\theta_{i0})}{E_0}(\Delta\epsilon + \Delta\epsilon_x), \tag{A18}$$

so that

$$S = 2\eta_x\int_{-t_0}^{t_0} dt g^2(z_t) + \frac{\sin^2(\theta_{i0})}{E_0}\Delta\epsilon \tag{A19}$$

and

$$S_c - S_s = 2\eta_x\int_{-t_0}^{t_0} dt\left[\cos\left(\frac{4\pi}{l}\frac{p_x}{M}t\right) - 2\sin^2(\theta_{i0})\right]g^2(z_t) - \frac{\sin^2(\theta_{i0})}{E_0}\Delta\epsilon_x, \tag{A20}$$

where $\Delta\epsilon$ and $\Delta\epsilon_x$ are given in Eqs. (2.29) and (2.30). Inserting all these results into the expression for the angular distribution as given in Eq. (A15) and integration over the variable $W$ gives the central expression for the angular distribution as given in Eqs. (2.45)–(2.47).

## APPENDIX B: THE JOINT ANGLE ENERGY DISTRIBUTION

In this Appendix we outline the derivation for the joint final angle and energy probability distribution. We first note the following thermal averages for the vertical and horizontal directions:

$$P(Y,A_x)=\left\langle \delta\left(Y-\frac{\Delta p_{x,2}}{p_z}-\mu\delta E_{B_x}\right)\delta(A_x-\mu\delta E_{B_x})\right\rangle_x$$
$$=\left(\frac{\beta|p_z|}{2M\mu l}\right)(H_{kk}H_{aa}-H_{ak}^2)^{-1/2}$$
$$\times\exp\left(-\frac{\beta\pi^2p_z^2}{M\mu^2l^2(H_{kk}H_{aa}-H_{ak}^2)}\right.$$
$$\times\left[(Y-A_x)^2\frac{\mu^2l^2}{4\pi^2}H_{aa}+A_x^2\frac{1}{p_z^2}H_{kk}\right.$$
$$\left.\left.-2(Y-A_x)A_x\frac{1}{p_z}\frac{\mu l}{2\pi}H_{ak}\right]\right), \tag{B1}$$

where we used the notation:

$$H_{kk}=\frac{1}{2}\sum_{j=1}^{N}\frac{c_{j_x}^2}{\omega_{j_x}^2}\left[X_{jc}^2\cos^2\left(\frac{2\pi}{l}x(t_0)\right)+X_{js}^2\sin^2\left(\frac{2\pi}{l}x(t_0)\right)\right]$$
$$=\frac{1}{2}\eta_x\int_{-t_0}^{t_0}dtg^2(z_t)+\frac{1}{2}\cos\left(\frac{4\pi}{l}x(t_0)\right)\eta_x$$
$$\times\int_{-t_0}^{t_0}dt\cos\left(\frac{4\pi p_x}{lM}t\right)g^2(z_t), \tag{B2}$$

$$H_{aa}=\frac{1}{2}\sum_{j=1}^{N}c_{j_x}^2\left[X_{js}^2\cos^2\left(\frac{2\pi}{l}x(t_0)\right)+X_{jc}^2\sin^2\left(\frac{2\pi}{l}x(t_0)\right)\right]$$
$$=\frac{4\pi^2}{Ml^2}\langle\Delta E_B\rangle_x, \tag{B3}$$

$$H_{ak}=\frac{1}{2}\sum_{j=1}^{N}\frac{c_{j_x}^2}{\omega_{j_x}}X_{js}X_{jc}=-\eta_x\frac{\pi}{l}\frac{p_x}{M}\int_{-t_0}^{t_0}dtg^2(z_t)=\frac{2\pi}{Ml}\Delta p_{x,1}. \tag{B4}$$

and

$$\mu=\frac{\tan(\theta_{i0})}{2E_0}. \tag{B5}$$

For the vertical direction we find

$$P(A_z)=\langle\delta(A_z-\delta E_{B_z})\rangle_z=\left(\frac{\beta}{4\pi\langle\Delta E_B\rangle_z}\right)^{1/2}\exp\left(-\frac{\beta A_z^2}{4\langle\Delta E_B\rangle_z}\right). \tag{B6}$$

The joint angle and energy distribution is then given as

$$P(\theta,E)=\frac{1}{l}\int_0^l dx(t_0)\int_{-\infty}^{\infty}dYdA_xdA_zP(A_z)P(Y,A_x)$$
$$\times\delta\left(\theta+\theta_{i0}+K(p_x,p_z)\sin\left(\frac{2\pi}{l}x(t_0)\right)+Y\right.$$
$$\left.+\frac{\Delta p_{x,1}}{p_z}+\mu\left(\langle\Delta E_B\rangle_z+\langle\Delta E_B\rangle_x+\frac{A_z}{\mu}\right)\right)$$
$$\times\delta\left(E-E_0+\langle\Delta E_B\rangle_z+\langle\Delta E_B\rangle_x+\frac{A_z+A_x}{\mu}\right). \tag{B7}$$

It is then a matter of carrying out the Gaussian integration over the variables $Y$, $A_x$, and $A_z$ to find the result:

$$P(\theta,E)=\frac{1}{l}\int_0^l dx(t_0)\int_{-\infty}^{\infty}dW\left(\frac{\beta|p_z|}{4\pi}\right)\left(\frac{1}{M(H_{kk}\langle\Delta E_B\rangle-\Delta p_{x,1}^2/M)}\right)^{1/2}\exp\left(-\frac{\beta}{4}\left[\frac{\Lambda^2MH_{kk}+\langle\Delta E_B\rangle p_z^2W^2+2\Lambda W\Delta p_{x,1}p_z}{M(H_{kk}\langle\Delta E_B\rangle-\Delta p_{x,1}^2/M)}\right]\right)$$
$$\times\delta\left(\theta+\theta_{i0}+K(p_x,p_z)\sin\left(\frac{2\pi}{l}x(t_0)\right)+W+\tan(\theta_{i0})\left[\frac{\Delta p_{x,1}}{p_x}-\frac{\Lambda-\langle\Delta E_B\rangle}{2E_0}\right]\right), \tag{B8}$$

where we used the shorthand notation

$$\Lambda=E-E_0+\langle\Delta E_B\rangle. \tag{B9}$$

## APPENDIX C: THE ANGLE DEPENDENT FINAL AVERAGE ENERGY

The joint probability distribution for finding a given value of the angle and final energy may be written as

$$P(\theta,E)=\frac{1}{l}\int_0^l dx(t_0)P(\theta,E,x(t_0)), \tag{C1}$$

where

$$P(\theta,E,x(t_0))=\int_{-\infty}^{\infty}dW\left(\frac{\beta|p_z|}{4\pi}\right)\left(\frac{1}{M(H_{kk}\langle\Delta E_B\rangle-\Delta p_{x,1}^2/M)}\right)^{1/2}\exp\left(-\frac{\beta}{4}\left[\frac{MH_{kk}\left(\Lambda+\frac{W\Delta p_{x,1}p_z}{MH_{kk}}\right)^2}{M(H_{kk}\langle\Delta E_B\rangle-\Delta p_{x,1}^2/M)}\right]\right)$$
$$\times\exp\left(-\frac{\beta p_z^2W^2}{4M}\right)\delta\left(\theta+\theta_{i0}+K(p_x,p_z)\sin\left(\frac{2\pi}{l}x(t_0)\right)+W+\tan(\theta_{i0})\frac{\Delta p_{x,1}}{p_x}-\frac{\tan(\theta_{i0})}{2E_0}(\Lambda-\langle\Delta E_B\rangle)\right) \tag{C2}$$

and $\Lambda$ is defined as in Eq. (B9). This implies that

$$\int_{-\infty}^{\infty} dEEP(\theta,E) = \frac{1}{l}\int_0^l dx(t_0)\int_{-\infty}^{\infty} d\Lambda P(\theta,\Lambda,x(t_0))[\Lambda + E_0 - \langle \Delta E_B\rangle] = E_0 P(\theta) + \frac{1}{l}\int_0^l dx(t_0)\int_{-\infty}^{\infty} d\Lambda P(\theta,\Lambda,x(t_0))(\Lambda - \langle \Delta E_B\rangle). \tag{C3}$$

We then note that

$$\int_{-\infty}^{\infty} d\Lambda P(\theta,\Lambda,x(t_0))\Lambda = -\frac{2}{\beta}\left[\langle \Delta E_B\rangle \frac{\tan(\theta_{i0})}{2E_0} + \frac{\Delta p_{x,1}}{p_z}\right]\frac{\partial}{\partial\theta}P(\theta,x(t_0)), \tag{C4}$$

where

$$P(\theta,x(t_0)) = \int_{-\infty}^{\infty} dEP(\theta,E,x(t_0)) = \frac{1}{\sqrt{\pi\Sigma^2}}\exp\left(-\frac{\left(\theta+\theta_{i0}+K(p_x,p_z)\sin\left(\frac{2\pi}{l}x(t_0)\right)+\Delta\theta_1(x(t_0))\right)^2}{\Sigma^2}\right). \tag{C5}$$

We then denote the averaging over the horizontal coordinate as

$$\langle f\rangle_l = \frac{1}{lP(\theta)}\int_0^l dx(t_0) f(x(t_0))P(\theta,x(t_0)), \tag{C6}$$

so that

$$\int_{-\infty}^{\infty} dEEP(\theta,E) = (E_0 - \langle\langle \Delta E_B\rangle\rangle_l)P(\theta) - \frac{1}{\beta}\frac{\partial}{\partial\theta}\left\langle P(\theta)\left[\langle \Delta E_B\rangle\frac{\tan(\theta_{i0})}{E_0} + 2\frac{\Delta p_{x,1}}{p_z}\right]\right\rangle_l, \tag{C7}$$

and this then gives Eq. (2.54).


[1] W. W. Hayes and J. R. Manson, Phys. Rev. B **75**, 113408 (2007).
[2] W. W. Hayes, H. Ambaye, and J. R. Manson, J. Phys.: Condens. Matter **19**, 305007 (2007).
[3] K. D. Gibson, S. J. Sibener, H. P. Upadhyaya, A. L. Brunsvold, J. Zhang, T. K. Minton, and D. Troya, J. Chem. Phys. **128**, 224708 (2008).
[4] D. Farías and K.-H. Rieder, Rep. Prog. Phys. **61**, 1575 (1998).
[5] B. Gumhalter, Phys. Rep. **351**, 1 (2001).
[6] R. Guantes, A. S. Sanz, J. Margalef-Roig, and S. Miret-Artés, Surf. Sci. Rep. **53**, 199 (2004); A. S. Sanz and S. Miret-Artés, Phys. Rep. **451**, 37 (2007).
[7] E. K. Schweizer and C. T. Rettner, Phys. Rev. Lett. **62**, 3085 (1989).
[8] E. K. Schweizer, C. T. Rettner, and S. Holloway, Surf. Sci. **249**, 335 (1991).
[9] K. H. Rieder and W. Stocker, Phys. Rev. B **31**, 3392 (1985).
[10] B. Berenbak, S. Zboray, B. Riedmuller, D. C. Papageorgopoulos, S. Stolte, and A. W. Kleyn, Phys. Chem. Chem. Phys. **4**, 68 (2002).
[11] H. J. Castejón, Surf. Sci. **564**, 165 (2004).
[12] A. Raukema, R. J. Dirksen, and A. W. Kleyn, J. Chem. Phys. **103**, 6217 (1995).
[13] C. T. Rettner, J. A. Barker, and D. S. Bethune, Phys. Rev. Lett. **67**, 2183 (1991).
[14] J. A. Barker, C. T. Rettner, and D. S. Bethune, Chem. Phys. Lett. **188**, 471 (1992).
[15] R. J. W. E. Lahaye, A. W. Kleyn, S. Stolte, and S. Holloway, Surf. Sci. **338**, 169 (1995).
[16] R. Brako, Surf. Sci. **123**, 439 (1982).
[17] T. C. M. Horn, A. W. Kleyn, and E. A. Gislason, J. Chem. Phys. **85**, 7388 (1986); A. W. Kleyn and T. C. M. Horn, Phys. Rep. **199**, 191 (1991).
[18] J. C. Tully, J. Chem. Phys. **92**, 680 (1990).
[19] T. Yan, W. L. Hase, and J. C. Tully, J. Chem. Phys. **120**, 1031 (2004).
[20] E. Pollak, S. Sengupta, and S. Miret-Artés, J. Chem. Phys. **129**, 054107 (2008).
[21] K. Imne, E. Ozizmir, M. Rosenbaum, and P. F. Zweifel, J. Math. Phys. **8**, 10907 (1967).
[22] E. J. Heller, J. Chem. Phys. **65**, 1289 (1981); E. J. Heller and R. C. Brown, *ibid.* **75**, 1048 (1976).
[23] H. W. Lee and M. O. Scully, J. Chem. Phys. **73**, 2238 (1980).
[24] V. S. Filinov, Yu. V. Medvedev, and V. L. Kamskyi, Mol. Phys. **85**, 711 (1995).
[25] E. Pollak and J. L. Liao, J. Chem. Phys. **108**, 2733 (1998).
[26] J. Shao, J.-L. Liao, and E. Pollak, J. Chem. Phys. **108**, 9711 (1998).
[27] H. B. Wang, X. Sun, and W. H. Miller, J. Chem. Phys. **108**, 9726 (1998).
[28] W. H. Miller, J. Chem. Phys. **125**, 132305 (2006).
[29] E. Pollak, H. Grabert, and P. Hänggi, J. Chem. Phys. **91**, 4073 (1989).